Metal-Induced Cyclization

A Unique Approach to Metal-Induced Bergman Cyclization: Long-Range Enediyne Activation by Ligand-to-Metal Charge Transfer**

Sibaprasad Bhattacharyya, Maren Pink, Mu-Hyun Baik, and Jeffrey M. Zaleski**

The development of stable enediyne constructs and subsequent low-temperature routes to Bergman-cyclized diradical formation are paramount for this class of molecule to realize its potential in biological applications. Metals have been shown to thermally activate stable enediynes by both σ-donor coordination[1–5] and π complexation,[6,7] which induce a marked reduction in the thermal barrier to Bergman cyclization. Despite these advances, the scope of the metal-activated Bergman cyclization remains poorly defined.

Electronic factors[8] that contribute to metal-centered enediyne activation are more elusive than the established influences of the geometry around the metal center.[1–5] Computational[9,10] and experimental[11] evaluations of the Bergman cyclization reaction coordinate show that σ acceptor/π donor functionalities at the alkyne termini reduce the activation barrier to diradical formation. In an effort to extend this model, we questioned whether binding of a strong Lewis acid in the vicinity of the alkyne termini would induce sufficient electron polarization to promote enediyne cyclization in an analogous manner. Herein, we report the preparation of Mo^{IV}–enedithiolate–enediyne complexes that show considerable differences in reactivity, which can be directly attributed to electron polarization rather than geometric effects of the metal center.

Reaction of 1,8-dibromooct-4-ene-2,6-diyne (**1a**) with the dicesium salt of 1,3-dithiole-2-thione-4,5-dithiolate (DMIT; **2**) generates **3a** in low (ca. 20%) yield (Scheme 1). Addition of **3a** to a stirred slurry of mercury(II) acetate in chloroform/acetic acid (3:1) affords the dithiol-2-one **4a** in 60% yield. The benzannulated counterpart **4b** was prepared analogously using 1,2-bis(3-bromopropynyl)benzene (**1b**) as the starting material. Compounds **4a** and **4b** are stable in solution and do not cyclize upon heating at 180°C in DMSO/1,4-cyclohexadiene (CHD; 1:100) over 12 h.

The dipotassium salt of enediyne ligand 3,10-dialkylthiacyclododec-1,6-ene-4,8-diyne-1,2-dithiolate (**5a**) was prepared by addition of two equivalents of EtOK to a slurry of **4a** in methanol to yield **5a** in situ as a light yellow solution (Scheme 2). The benzannulated dipotassium salt **5b** was prepared in the same manner from **4b**. Both **5a** and **5b** are stable at ambient temperature in methanol under nitrogen for 3 hours, and at 80°C for 1.5 hours, prior to slow decomposition to non-Bergman side products.

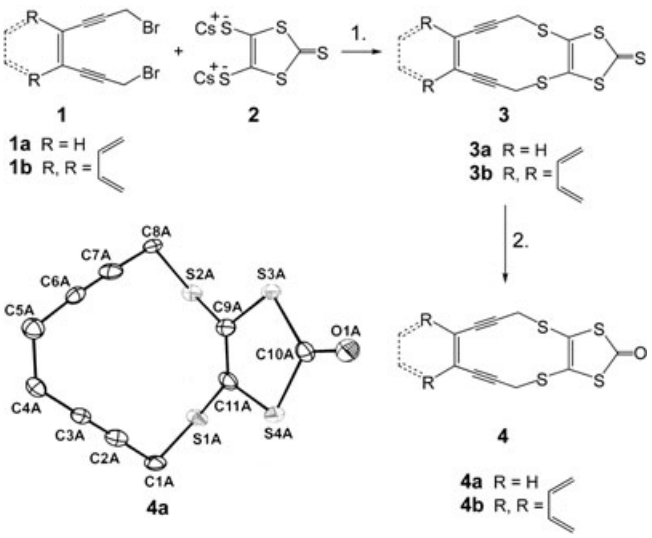

Scheme 1. Synthesis and X-ray structure of **4** (40% probability). 1) MeOH, 0°C, 12 h, 20%; 2) $CHCl_3$/AcOH (3:1), $Hg(OAc)_2$, RT, 12 h, 60%.

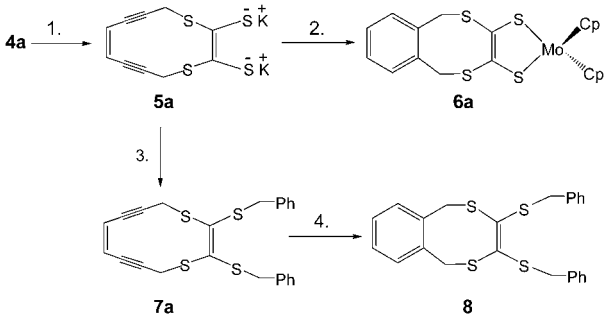

Scheme 2. Bergman cyclization of **5a** and thermal reactivity of **7a**. 1) MeOH, KOEt (2 equiv), RT, 15 min; 2) $[MoCp_2Cl_2]$, CHD, 60°C, 30 min, 40%; 3) $PhCH_2Br$, 25°C, 80%; 4) DMSO, CHD, 180°C, 24 h, 60%.

Heating of **5a** in the presence of dichlorobis(η^5-cyclopentadienyl)molybdenum(IV) in methanol/CHD (1:100) at 60°C for 0.5 h affords the Bergman-cyclized product **6a** in approximately 40% yield, with the remaining mass balance consisting of insoluble polymeric materials common to Bergman cyclization reactions. No metal complexation or product formation are observed at lower temperatures, while decomposition occurs without an increase in product yield at higher temperatures. The X-ray structure of **6a** (Figure 1) exhibits a pseudo-tetrahedrally coordinated Mo^{IV} center with two thiolate ligands from the enediyne chelate and two η^5-cyclopentadienyl (Cp) rings bound in the plane perpendicular to the enedithiolate core. The newly formed aromatic ring is

[*] S. Bhattacharyya, M. Pink, Prof. M.-H. Baik, Prof. J. M. Zaleski
Department of Chemistry
Indiana University
800 E. Kirkwood Avenue, Bloomington, IN 47405 (USA)
Fax: (+1) 812-855-8300
E-mail: mbaik@indiana.edu
zaleski@indiana.edu

[**] The support of the National Institutes of Health (R01 GM62541-01) and the National Science Foundation (0116050) is gratefully acknowledged.

Supporting information for this article is available on the WWW under http://www.angewandte.org or from the author.

  DOI: 10.1002/anie.200461825

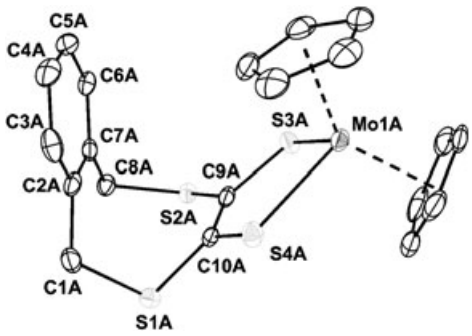

Figure 1. X-ray structure of **6a**. Thermal ellipsoids are illustrated at 40% probability.

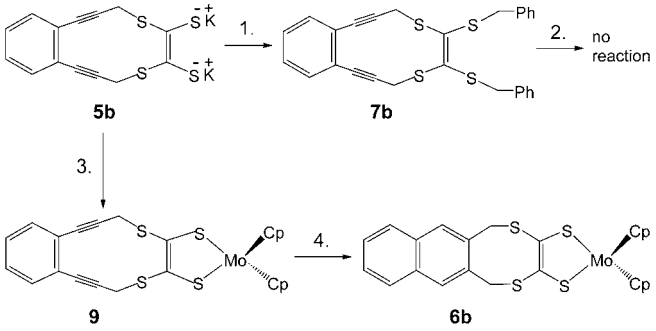

Scheme 3. Contrasting reactivities of **7b** and **9**. 1) $PhCH_2Br$, 25 °C, 80%; 2) DMSO, CHD, 180 °C, 24 h; 3) MeOH, $[MoCp_2Cl_2]$, 60 °C, 30 min, 42%; 4) DMSO, CHD, 120 °C, 5 h, 15%.

poised above the Mo–S_2C_2 plane as a consequence of the two pairs of sp^3 sulfur and carbon atoms between the metal–enedithiolate and aromatic substructures.

To evaluate whether σ coordination or π complexation promoted the cyclization reaction, **5a** was benzylated to **7a** by reaction with benzyl bromide (Scheme 2). Compound **7a** is highly stable, but can be cyclized to **8** in 60% yield by heating in solution (DMSO/CHD, 1:100) for 24 h at 180 °C. In contrast, the refluxing of **7a** with $[MoCp_2Cl_2]$ in methanol/THF solution at 60 °C in the presence of excess CHD results in no reaction, thereby disqualifying a π interaction between the enediyne fragment and molybdenum as the origin of enediyne activation. DFT calculations[12] confirm the enhancement in reactivity by molybdenum complexation, and predict an activation enthalpy of 17.7 kcal mol^{-1} to give the transition state **7c-TS**, whereas the transition state **7a-TS** for the benzylated analogue **7a** has an activation enthalpy of 21.9 kcal mol^{-1}. The structures of the transition states are analogous to that previously described elsewhere for a prototype reaction.[13] These activation parameters are in excellent agreement with the kinetics for conversion of **5a**→**6a** ($\Delta H^{\neq} = 14.25$ kcal mol^{-1}; $\Delta S^{\neq} = -31.52$ eu). Since cyclization of **7a**→**8** requires heating between 150 °C (no reaction) and 180 °C (24 h, 60%), the reaction barrier is estimated from a simple Arrhenius proportion to be 3–5 kcal mol^{-1} higher than that for formation of **6a**, which is also in good agreement with the trend of the calculated enthalpies of activation for these compounds.

Parallel reactions were performed with the benzannulated ligand **5b**, which is thermally more stable toward Bergman cyclization than **5a** as a result of the higher endothermicity of the Bergman reaction, which makes the retrocyclization competitive with H-atom abstraction.[14,15] Within this theme, heating of benzylated derivative **7b** (prepared in an analogous manner to **7a**) at 180 °C for 24 h in DMSO/CHD (1:100) results in no reaction, which reflects the added enediyne stability introduced by benzannulation (Scheme 3). As a consequence of the enhanced stability and in contrast to the reactivity of **5a**, reaction of **5b** with $[MoCp_2Cl_2]$ at 60 °C for 0.5 h gives the uncyclized enediyne complex **9** in 42% yield. Subsequent heating of **9** at 120 °C for 5 h activates the ligand and generates Bergman-cyclized product **6b** in 15% yield, with considerable recovery of starting material (60%). Heating at higher temperatures leads to gradual decomposition of both starting material and cyclized product. The X-ray structures of metalloenediyne **9** and cyclized product **6b** (Figure 2) reveal similar pseudo-tetrahedral structures to that of **6a**. The separations of the alkyne termini (C2···C7) in **4a** and **9** are identical (4.05 Å), which suggests an electronic rather than a geometric origin for the observed cyclization temperatures. Consistent with this premise, Mo^{IV} complexes **6a**, **6b**, and **9** show characteristic $S \rightarrow Mo^{IV}$ ligand-to-metal charge-transfer transitions between 500 and 535 nm with significant molar extinction coefficients of $\varepsilon \approx 1300$–1700 M^{-1} cm^{-1} (Figure 3).

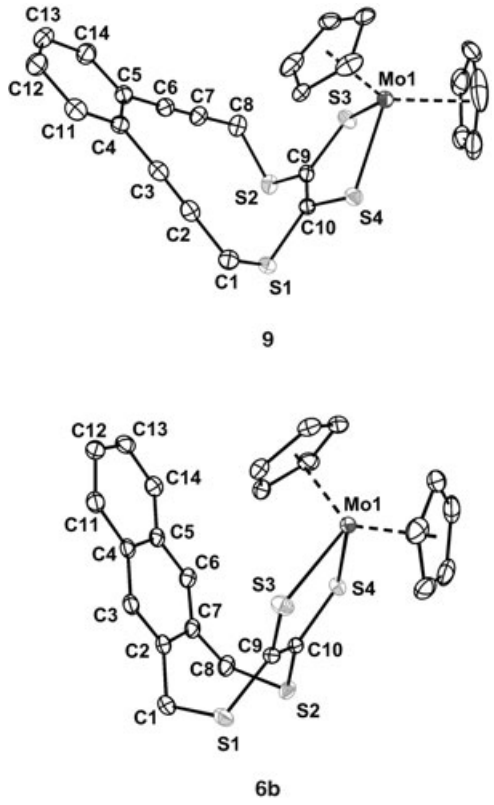

Figure 2. X-ray structures of metalloenediyne **9** and subsequent cyclized product **6b**. Thermal ellipsoids are illustrated at 40% probability.

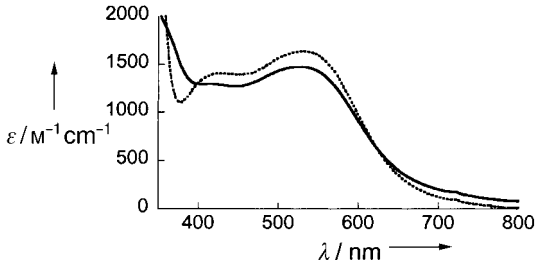

Figure 3. Electronic spectra of **9** (——) and **6b** (-----) in CH_2Cl_2.

To quantify the polarization effect, we examined the partial charges derived from our DFT-computed total densities (Figure 4) for cyclization of benzylated ligand **7a**→**7a-TS** and Mo complex **7c**→**7c-TS**. For the **7a**→**7a-TS** transformation, the enediyne carbon atoms C2 and C7 which form the developing σ bond become positively polarized by as much as 0.3–0.4 electron units as a result of the change in hybridization from sp^1 to sp^2, while C3 and C6 become the centers of the diradical electrons and are consequently negatively polarized. Complexation of the $\{MoCp_2\}$ fragment reduces the amplitudes of these differential charges at C2,C7 and C3,C6 notably for progression from **7c** to **7c-TS** (for example, the differential charges at C2 for **7a**→**7a-TS** and **7c**→**7c-TS** are 0.29 and 0.08, respectively), thus indicating a net delocalization of charge upon metal complexation, which lowers the energy of the cyclization transition state by reducing charge repulsion. This concept is a logical extension of a previously suggested mechanism that considered delocalization through hyperconjugation and electron repulsion as key contributions to the energy barriers for Bergman cyclization.[16–18]

In addition to the metal-induced electrostatic contribution to the disparate reactivities of **7a** and **7c**, there is superimposed a more complex ensemble of orbital effects that also supports a decrease in the activation barrier upon Lewis acid (for example, Mo^{IV}) complexation. The first consequence of metal binding is a lowering of the symmetric and antisymmetric enedithiolate orbitals by bonding interactions with the effective d_{z^2} and d_{xy} orbitals, respectively (see Supporting Information). Second, the molecular orbitals (MOs) involved in the formation of the developing C2–C7 σ bond, the in-phase and out-of-phase combinations of the in-plane π orbitals of the diyne (MO-104/MO-107 and MO-99/MO-101 of **7a** and **7c**, respectively; Figures 5 and 6), display no direct electronic interaction of the Mo center with the π orbitals, which suggests that the function of the metal center reported here may be general and valid for any Lewis acid. Third, comparison of the shapes of the two π MOs of **7a** and **7c** reveals that the disposition of the S-based lone-pair orbitals to

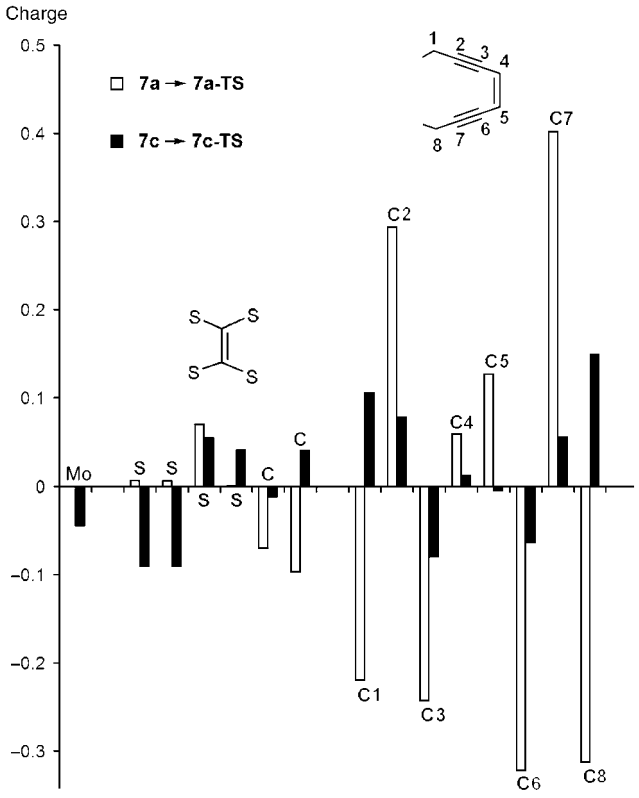

Figure 4. Partial charge changes accompanying the formation of the respective transition states. Charges are derived from fits of the electrostatic potential generated by the DFT-computed total electron densities.

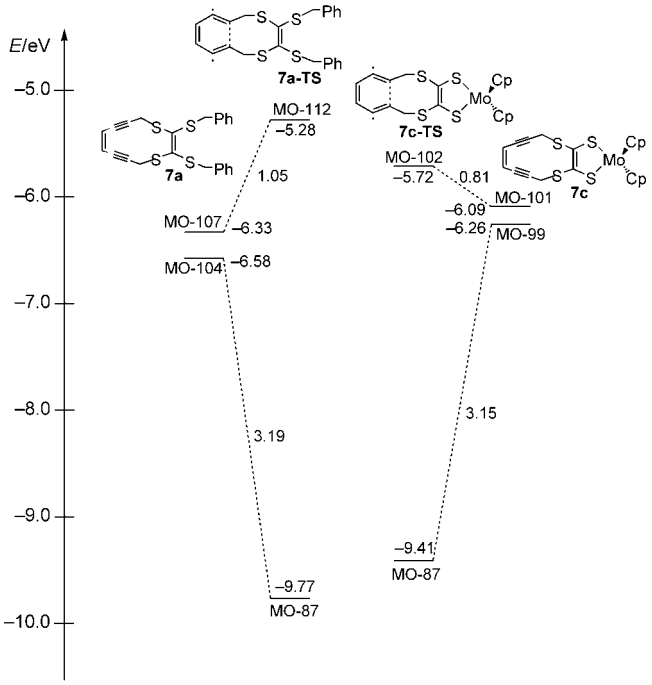

Figure 5. MO diagram illustrating the relative energy changes of the two most important MOs that promote C–C bond formation between the ground and transition states for the benzylated and metal-substituted enediynes, respectively. Orbital energies are indicated in eV.

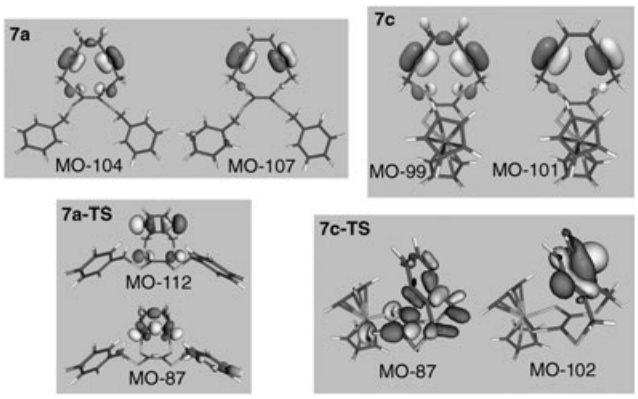

Figure 6. Isosurface plots (0.05 a.u.) of the most important MOs that are also illustrated in Figure 5.

lower energies by Mo complexation allows them to more efficiently mix with the diyne-based π orbitals. This differential polarization effect is strongly pronounced in the transition states; MO-87 of the metal complex (**7c**-**TS**) shows substantially more S character than the corresponding MO-87 of the benzylated ligand (**7a**-**TS**). Interestingly, this mixing has only a modest influence on the energy change of these MOs (Figure 5). Upon formation of **7a**-**TS**, MO-104 of **7a** becomes stabilized by 3.19 eV to give MO-87 of **7a**-**TS**, compared to the essentially identical stabilization of MO-99 in **7c** (3.15 eV) to give MO-87 in **7c**-**TS**. Thus, binding of the Lewis acid has only a minor impact on the energetics of σ-bond formation. However, the Mo center stabilizes the diradicaloid transition state by lowering the energy of MO-102 in **7c**-**TS** by 0.44 eV relative to its analogue MO-112 in **7a**-**TS**. This effect derives from the fact that MO-102 of **7c**-**TS** is characterized by a localized diradical, where electron density arising from a lone pair of electrons on the sulfur atom that could contribute to electron–electron repulsion in the transition state has been energetically removed by metal complexation. In contrast, MO-112 of **7a**-**TS** reveals participation of the electron density from the lone pair of electrons on the sulfur atom in the diradicaloid orbital of the transition state, which causes a net destabilization and concomitant decrease in thermal reactivity.

Summarizing the electronic structure origin of the differential reactivity of **7a** and **7c**: 1) many orbitals show σ-bond polarization upon metal complexation without a single dominant contribution; 2) net polarization caused by Mo^{IV} complexation delocalizes enediyne electron density and simultaneously removes charge repulsion in the 1,4-diradical orbital of the transition state; and 3) the net polarization effect on enediyne reactivity is likely transferable to other metal–enediyne motifs. More generally, we have demonstrated that high-valent metals can be effective cofactors for enediyne activation through electronic rather than geometric influences.

Received: August 30, 2004
Published online: December 7, 2004

Keywords: charge transfer · cyclization · enediynes · molybdenum · radicals

[1] B. P. Warner, S. P. Millar, R. D. Broene, S. L. Buchwald, *Science* **1995**, *269*, 814 – 816.
[2] B. Konig, W. Pitsch, I. Thondorf, *J. Org. Chem.* **1996**, *61*, 4258 – 4261.
[3] A. Basak, J. C. Shain, *Tetrahedron Lett.* **1998**, *39*, 3029 – 3030.
[4] P. J. Benites, D. S. Rawat, J. M. Zaleski, *J. Am. Chem. Soc.* **2000**, *122*, 7208 – 7217.
[5] D. S. Rawat, J. M. Zaleski, *J. Am. Chem. Soc.* **2001**, *123*, 9675 – 9676.
[6] J. M. O'Connor, L. I. Lee, P. Gantzel, A. L. Rheingold, K.-C. Lam, *J. Am. Chem. Soc.* **2000**, *122*, 12057 – 12058.
[7] J. M. O'Connor, S. J. Friese, M. Tichenor, *J. Am. Chem. Soc.* **2002**, *124*, 3506 – 3507.
[8] S. Bhattacharyya, A. E. Clark, M. Pink, J. M. Zaleski, *Chem. Commun.* **2003**, 1156 – 1157.
[9] N. Koga, K. Morokuma, *J. Am. Chem. Soc.* **1991**, *113*, 1907 – 1911.
[10] M. Prall, A. Wittkopp, A. A. Fokin, P. R. Schreiner, *J. Comput. Chem.* **2001**, *22*, 1605 – 1614.
[11] M. Nath, J. C. Huffman, J. M. Zaleski, *J. Am. Chem. Soc.* **2003**, *125*, 11484 – 11485.
[12] Calculations were carried out using Jaguar 5.5 (Schrödinger, Inc.) at the BPW91/6-31G**++ level of theory; the LACVP**++ basis set was utilized for Mo. Transition states were confirmed by vibrational frequency calculations.
[13] C. J. Cramer, *J. Am. Chem. Soc.* **1998**, *120*, 6261 – 6269.
[14] S. Koseki, Y. Fujimura, M. Hirama, *J. Phys. Chem. A* **1999**, *103*, 7672 – 7675.
[15] T. Kaneko, M. Takahashi, M. Hirama, *Tetrahedron Lett.* **1999**, *40*, 2015 – 2018.
[16] I. V. Alabugin, M. Manoharan, *J. Phys. Chem. A* **2003**, *107*, 3363 – 3371.
[17] I. V. Alabugin, M. Manoharan, S. V. Kovalenko, *Org. Lett.* **2002**, *4*, 1119 – 1122.
[18] I. V. Alabugin, T. A. Zeidan, *J. Am. Chem. Soc.* **2002**, *124*, 3175 – 3185.

